Tanzania Journal of Science 48(4): 727-740, 2022
ISSN 0856-1761, e-ISSN 2507-7961

Performance Investigations of the Charging and Discharging Processes in a 3-Tank Thermal Energy Storage System

Swaleh Tusiime[1*], Karidewa Nyeinga[1], Denis Okello[1] and Ole J. Nydal[2]
[1]*Department of Physics, Makerere University, P.O. Box 7062 Kampala, Uganda.*
[2]*Department of Energy and process Engineering, NTNU, P.O. Box 7491, Trondheim, Norway.*
[*]*Corresponding author, email: tsmswlh2@gmail.com*
Received 6 Sep 2022, Revised 31 Oct 2022, Accepted 13 Nov 2022, Published Dec 2022
DOI: https://dx.doi.org/10.4314/tjs.v48i4.1

Abstract

The paper presents a 3-tank thermal energy storage system. The system consists of cold oil reservoir, heat storage tank, and a residual drainage tank. Cold oil flows by gravity into a heating chamber and after being heated to the required temperature, a mechanical thermostat opens allowing the hot oil to flow into a heat storage tank. The storage tank was discharged through the cooking unit by boiling 0.5 litres of water. The used oil flowed by gravity to the drainage tank. The discharge flow rates of 0.5, 2.1, 2.8 and 6.5 g/s were considered. A charging efficiency of 51.3% and overall discharging efficiency range of 15.3–34.7% were achieved. Charging efficiency increased when the source was embedded in the storage tank. The instantaneous discharge power had a peak value for each flow rate. The adopted cooking unit had a thermal transfer efficiency range of 34.7–57.6%. A method for sizing oil based TES systems was proposed and illustrated based on the obtained discharge results.

Keywords: 3-tank, sizing, discharging, efficiency, thermal energy.

Introduction

Cooking energy is a challenge all over the world especially in developing countries (Gadonneix et al. 2010). The use of biomass has led to the high rate of deforestation and green-house gas emissions which contributes to global warming (Hassan and Hertzler 1988). In Uganda, the energy situation shows that cooking contributes about 90% of all household energy consumption (Lee 2013). The extraction of this energy is usually by inefficient burning of solid fuels on an open fire or traditional cooking stoves (Geller 1982). Therefore, there is need to provide clean, affordable, reliable energy for cooking in developing countries and to ensure efficient energy transfer or utilization processes (Fay et al. 2000, Rehfuess and WHO 2006).

Of the available energy sources (geothermal energy, hydropower, solar, wind, biomass and petroleum products), solar energy stands out as clean and freely available all over the Earth's surface during sunny hours of the day. For cooking purposes, solar energy is stored in thermal form. Indirect solar cookers use Thermal Energy Storage (TES) systems to store thermal energy for later use in the absence of sunshine (Dincer 1999, Panwar et al. 2012, Duffie and Beckman 2013).

The use of TES systems involves thermally charging it during periods of energy availability and extracting the thermal energy from it, when either the energy source is not available or when the energy demand is high. A TES system is charged by moving hot oil through the thermal energy source to the TES system either in a closed circuit where an oil pump is required (Mussard and Nydal 2013, Okello et al. 2016, Lugolole et al. 2018) or directly by free flow (Nkhonjera et al. 2017, Tabu et al. 2018, Kajumba et al. 2020).

More useful thermal energy is extracted from a sensible TES system when it is thermally stratified (Haller et al. 2009). Thermal stratification of a TES system is enhanced when charged at a constant temperature and this requires a thermostat. Mechanical thermostats available on the market have plastic and electronic components that cannot withstand high temperatures encountered in TES systems (200–350 °C). Hence there is need to use purely mechanical thermostats for TES systems.

In addition to ensuring thermal stratification, heat losses need to be minimized by selecting appropriate insulating material from those available on the market (Villasmil et al. 2019) and keeping the thermal source much closer to the TES system. This is to ensure that the charged TES system can be used to cook a meal within at least 24 hours. A simple standalone TES system that meets such conditions requires: a minimum of 3 oil tanks (for storing: the cold oil, the hot oil and the used oil), a temperature-controlled charging mechanism and an energy efficient cooking unit.

The study was aimed at constructing and evaluating the performance of the 3-tank TES system for cooking applications. The system should be able to take hybrid heat sources. The objectives of the study were:

1. To construct the proposed 3-tank TES system.
2. To test the charging and discharging processes and measure the corresponding efficiencies for the 3-tank TES system.
3. To assess the energy transfer processes or efficiencies involved.
4. To design and demonstrate an appropriate method of sizing this 3-tank oil-based TES system based on its results.

Materials and Methods

The schematic diagram in Figure 1A shows the major components of this 3-tank TES system: the cold oil reservoir, the thermostat, the storage tank, the cooking unit and the drainage tank.

Design, construction and assembly of the mechanical thermostat

Figure 1B shows the schematic diagram of the mechanical thermostat. The thermostat acts as a valve that is always closed and only opens when the temperature of the oil in it exceeds the preset value. It is composed of: the expansion system, the heating chamber and the slider-valve. The expansion system creates a force that moves through a displacement due to a temperature change. The expansion system was a copper coil locked at one end with a tap, gas welded to the pneumatic cylinder at the other end and filled with air-free expansion oil. The heating chamber was constructed by welding a mild steel sheet into a rectangular based cylinder open at the top and closed at the bottom. Two holes were drilled on the sides of the heating chamber: one near the bottom and the other near the top for coil-oil inlet and hot-oil outlet, respectively. An industrial standard heater 800 W 220 VAC was fixed at the bottom of the chamber near the cold oil inlet point using a mechanical drill. Part of the copper coil was dipped in the top oil in the heating chamber to act as a temperature sensor. The slider-valve was a sliding mechanism that opens and closes a pipe when the oil in the expansion system expands and contracts, respectively. The slider-valve was constructed such that it is always closed and only opens when the sliding-rod moved by the piston-rod of the pneumatic cylinder moves beyond a certain limit. The sliding valve was gas welded along the hot-oil pipe from the mechanical thermostat to the storage tank. This mechanical thermostat regulates the charging temperature by the opening and closing of the slider-valve using the expansion system so that only hot oil at a constant temperature is let into the storage tank. Table 1 provides the dimensions of the expansion system, the pneumatic cylinder and the heating chamber. The constructed mechanical thermostat was positioned between the cold oil reservoir and the storage tank as shown in Figure 1A.

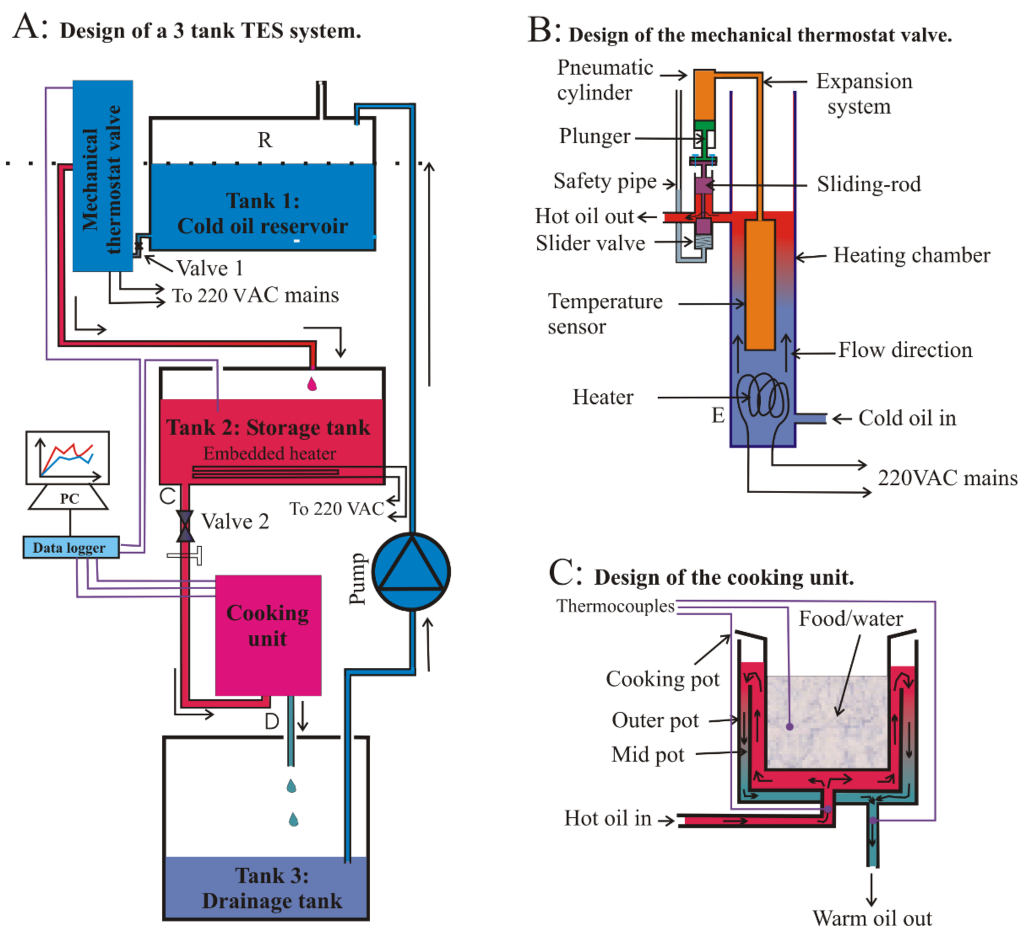

Figure 1: The schematic design of: A) the 3-tank TES system B) the mechanical thermostat and C) the cooking unit.

Table 1: Dimensions of the mechanical thermostat components

Heating chamber		Pneumatic cylinder		Expansion system	
Height	50.0 cm	Stroke length	5.0 cm	Length of copper coil	4.0 m
Width	4.0 cm	Diameter	2.5 cm	Diameter of copper coil	7.1 cm
Length	8.0 cm				

Design, construction and assembly of the cooking unit

The schematic diagram in Figure 1C shows the design of the cooking unit adopted from previous studies (Sjogren and Steen 2018, Kajumba et al. 2020). The 3 pots in the cooking unit were constructed from 1 mm thick mild steel into cylindrical pans with the dimensions shown in Table 2. Five holes of 6 mm in diameter were drilled equally spaced along the circumference of the mid pot at a height of 5 cm from its base. A 2 cm hole was drilled at the center of the mid pot and the outer pot. A hole 1 cm in diameter to let oil out of the cooking unit was drilled at the bottom of the outer-pot at a point, beyond the diameter of the mid pot. The mid pot was welded into the outer pot ensuring they are aligned centrally. The oil pipe from the storage tank was welded at this central hole to allow hot oil into the cooking unit. The smaller pan (cooking pot) sits in the two welded pans. The oil from the storage tank enters the cooking unit from the bottom of the cooking pot and rises to pass through the five holes in the mid pot into the outer-pot hence pouring out to the drainage tank. The cooking pot sits on top of the incoming oil. The arrows in the cooking unit in Figure 1C show the directions of oil flow during the discharge process.

Design, construction and assembly of the 3-tank TES system

The cold oil reservoir was made by electrically welding a mild-steel sheet into a cylinder open at one end and closed at the other end. A galvanized pipe (with internal diameter of 1.3 cm) was connected from the bottom of the oil reservoir to the bottom of the heating chamber by electrical welding. Valve 1 was fixed along this galvanized pipe so as to stop oil flow from the cold oil reservoir whenever necessary. A similar insulated galvanized pipe was connected from near the top of the mechanical thermostat to the top of the storage tank. The storage tank was constructed by electrically welding a mild-steel sheet into a cylinder closed at both ends. Two holes were drilled at the top side of the storage tank, one for hot oil inlet and the other for the thermocouple. A pipe 1.6 cm in internal diameter was gas-welded from the bottom of the storage tank to the cooking unit with valve 2 along it. A heater 4000 W 220 VAC was embedded at the bottom of the storage tank by cutting a part of the storage tank casing, fixing the heater on it and gas welding that part back. The drainage tank was constructed by welding mild steel into a cylinder closed at the bottom and open at the top. The drainage tank was positioned below the cooking unit to receive and store the used oil from the cooking unit. The storage tank, cooking unit and the piping between the two, were insulated using rock wool insulation blanket. The dimensions of the 3-tanks are provided in Table 2**.** K-type thermocouples were positioned to measure the temperature of oil: from the mechanical thermostat, in the storage tank, to and from the cooking unit and the temperature of water in the cooking pot. The temperature recording system was controlled by the Picotech Data logger system that generates temperature-time series files on a computer. Shell thermia B oil (BPS Shell 2021) was used throughout this experiment as: a heat transfer fluid, a heat storage material and as a thermal-expansion liquid in the expansion system. Figure 2 shows the photograph of the fully assembled experimental setup for the 3-tank TES system.

Table 2: The dimensions of the 3-tanks in the TES system and the 3 pots in the cooking unit: H is Height and D is Diameter.

	The 3–Tanks in the TES system			The 3 pots in the cooking unit		
	Reservoir tank	Storage tank	Drainage tank	Outer pot	Mid pot	Cooking pot
H (cm)	36.5	62.1	36.0	11.0	7.0	6.0
D (cm)	39.1	20.1	37.1	18.5	15.5	14.0

During charging: oil from the cold oil reservoir flows by gravity to the thermostat when valve 1 is open. The storage tank receives hot oil at an averagely constant charging temperature until when it is sufficiently thermally charged. With valve 1 closed, the charged storage tank discharged through the cooking unit by opening valve 2. The degree of opening of valve 2 determines the discharge flow rate.

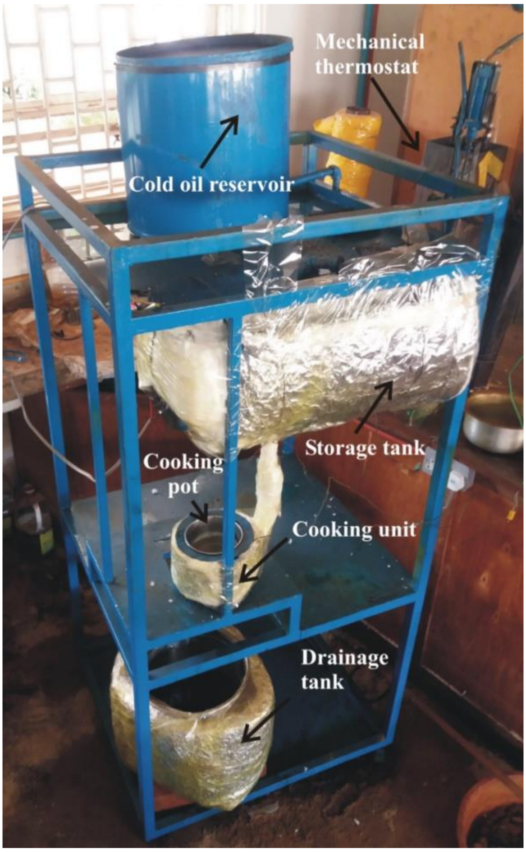

Figure 2: The photograph of the experimental setup for the 3-tank TES system.

Charging and discharging the 3-tank TES system

The 3-tank TES system was thermally charged using the mechanical thermostat to obtain the results in Figure 3. The height of oil in the cold oil reservoir measured using a dip-stick reduced from 20.0 cm to 14.3 cm in 1 hour during this charging process. For comparative charging purposes, 32 litres of oil in the storage tank were heated directly using the embedded heater to the smoke point (~ 240 °C) as shown in Figure 4. While using the embedded heater, valve 1 was closed and the heater in the thermostat was switched off. Figure 5 shows the cooling thermal profile for the reheated 32 litres of oil. The storage tank was discharged through the cooking unit by opening valve 2 at the mass flow rates of 0.5 g/s, 2.1 g/s, 2.8 g/s and 6.5 g/s. The mass flow rates were estimated as the ratio of the oil mass collected flowing from the cooking unit to the time taken to collect it. Figure 6 shows the temperature profiles during the discharge process for each mass flow rate.

Parameters and equations to characterize the charging and discharging processes

The thermal energy in the oil

The quantity of thermal energy E stored in oil that has been heated from a temperature T_o to temperature T is given by equation (1) (Fernandez-Seara et al. 2007).

$$E = c_{av}\,\rho_{av}\,V\,\left(T - T_o\right) \qquad (1)$$

where c_{av}, ρ_{av}, T and V are the average specific heat capacity, average density, average temperature, and volume of the oil being heated, respectively. c_{av} and ρ_{av} are functions of the average oil temperature and for Shell thermia B oil, they are given by equations (2) and (3), respectively (Mawire et al. 2014, Tabu et al. 2018).

$$c_{av}\left(T\right) = 0.0036T + 1.8087 \text{ J/gK} \quad (2)$$

$$\rho_{av}\left(T\right) = -0.0006T + 0.8748 \text{ g/cm}^3 \quad (3)$$

Equation (1) can be modified to give the oil quantity in terms of oil mass, *m*, by replacing the product of *V* and $\rho_{av}\left(T\right)$ in equation (1) by the mass *m* of the oil.

The discharge thermal power

The thermal power, P_{out}, absorbed by the cooking unit from the hot oil flowing through it from the storage tank is given by equation (4) (Incropera et al. 2007, Mawire et al. 2010).

$$P_{out} = c_{av}\,\rho_{av}\,v_{disc}\left(T_{in} - T_{out}\right) \quad (4)$$

where v_{disc}, T_{in} and T_{out} are the discharge volume flow rate, temperature of the hot oil flowing to the cooking unit and temperature of the oil leaving the cooking unit to the drainage tank.

In estimating c_{av} and ρ_{av}, the average temperature, T of T_{in} and T_{out} was used.

Heat loss to the ambient

According to Newtons's law of cooling , the thermal power loss to the ambient from a given hot body is given by equation (5) (Duffie and Beckman 2013)

$$\text{Power loss} = hA_s\left(T - T_a\right) \quad (5)$$

Where *h* is the heat transfer coefficient and A_s is the surface area of the body. The values of h and A_s vary depending on the surface design of the body.

Results and Discussion

The charging temperature profiles and efficiency

Figure 3 shows the temperature profiles obtained during the charging process using a mechanical thermostat.

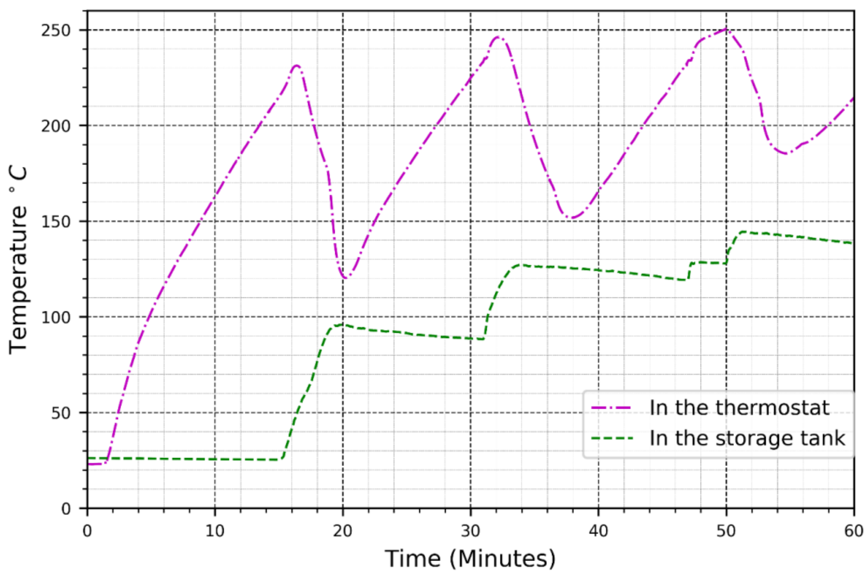

Figure 3: The temperature profile of oil in the thermostat and in the storage tank during the charging process using a mechanical thermostat.

Figure 3 shows that the temperature of the top oil in the thermostat increases from 25 °C to 230 °C due to the thermal energy supplied by the heater E. After the initial opening of the slider-valve after 16 minutes, the thermostat oil temperatures oscillate between 120 °C to 250 °C due to the opening and closing of the slider valve. The temperature range through which they oscillate, decreases with charging time from 110 °C to 65 °C in 40 minutes. The oil temperature in the storage tank increases stepwise from 30 °C to 140 °C in 1 hour. Oil temperature in the storage tank increased whenever the slider valve opened to let in hot oil. After a small quantity of hot oil had dropped in the storage tank, the oil temperature decreased slightly due to thermal loss to the storage tank metal casing.

The height of oil in the cold oil reservoir reduced from 20 cm (24 litres) to 14.3 cm (17.2 litres) in 60 minutes during the charging process. The 6.8 litres of oil from the cold oil reservoir, while at 140 °C in the storage tank contained 0.41 kWh of thermal energy. Since a 800W heater switched on for 60 minutes delivers 0.8 kWh, this leads to a charging efficiency of 51.3%. This efficiency can be improved by using a higher thermal power source with an improved insulation and reducing the size of the heating chamber. Most of the heat losses occur during thermal transfer from the source to the storage tank. Therefore, during charging, the available thermal energy should be transferred to the storage tank in the shortest possible time to minimize thermal losses. By having the thermal source in the storage tank, such thermal losses are eliminated. Figure 4 shows the average temperature profile at a point in the storage tank while directly heating the oil in it using the embedded heater.

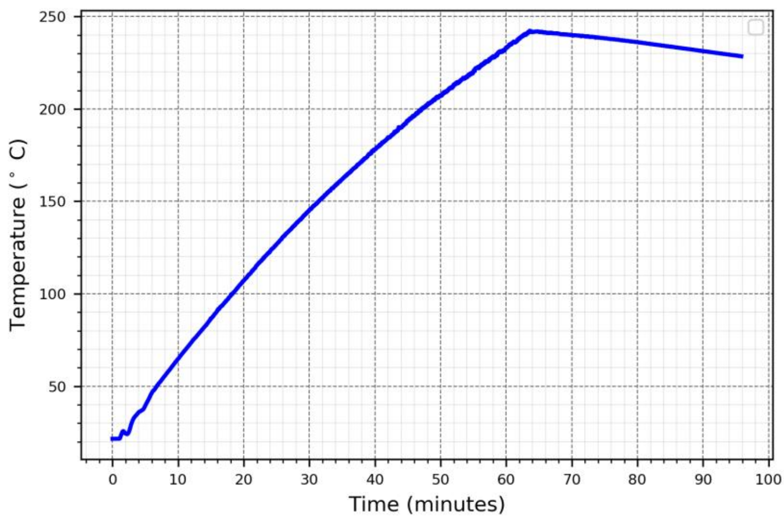

Figure 4: Charging temperatures in the 3-tank TES system using the embedded heater.

Figure 4 shows that the temperature at that point in the storage tank increased from 23 °C to 242 °C in 64 minutes due to the supplied thermal energy. On switching off the heater, the temperature decreased to 230 °C in the next 32 minutes due to thermal losses to ambient.

Of the 4.27 kWh supplied by the 4000 W heater in 64 minutes only 3.84 kWh got stored in the 32 litres of oil at 242 °C leading to a charging efficiency of 90%. This shows that there is an improvement in the charging efficiency from 51.3% to 90% when the energy source is within the TES system. Direct heating leads to thermal currents in the storage tank as hot oil rises to the top due to density difference and this destroys its thermal stratification.

Cooling test on the storage tank

For a steady cooling process, the oil in the storage tank was reheated and the cooling curve recorded as shown in Figure 5.

Figure 5 shows that the temperature of oil in the storage tank decreased from 268 ℃ to 100 ℃ in 17 hours which confirms that cooking cannot be achieved throughout the 24 hours. Therefore, there is need to: improve on the thermal insulation of the storage tank, ensuring that it is made from a material that is less conducting other than metal sheets and it could be disengaged from the other components like the cooking unit when not in use. *The perfectness of an insulation is reflected by* the value of its heat transfer coefficient. By equating the time rate of change of equation (1) to equation (5), it can be shown theoretically that the slope of the lower graph in Figure 5 is equal to the ratio $\frac{hA_s}{mc_{av}}$. The slope of this lower graph in Figure 5 was estimated as 0.064 per hour, A_s as 4553.6 cm^2 using the values in Table 2, c_{av} as 2.36 J/gk using equation (2) and mass of the oil in the storage tank was estimated as 25.1 kg from the oil volume using equation (3). Using these values, the heat transfer coefficient was estimated at 0.23 W/m^2k. Previous studies have obtained a slightly higher heat transfer coefficient of 0.54 W/m^2 for a cooking unit (Kajumba et al. 2020). The cooling test on the storage tank shows that its insulation needs to be improved so as to be able to cook after 24 hours.

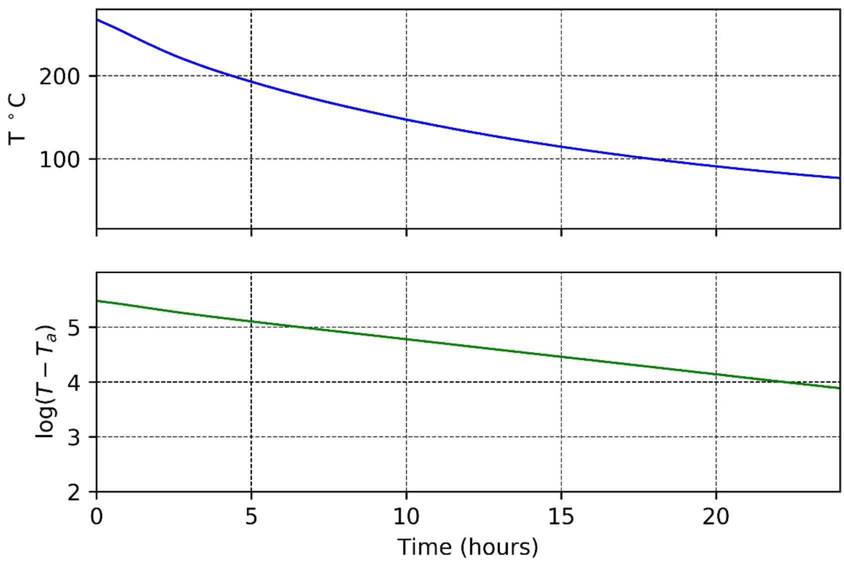

Figure 5: The cooling profile at the center of the hot oil stored in the storage tank.

The discharging temperature profiles

Figure 6 shows the temperature profiles at 4 points on a thermally charged 3-tank TES system for the discharge mass flow rates of 0.5, 2.1, 2.8 and 6.5 g/s. Figure 6 shows that the temperatures in the storage tank decreases for each flow rate during the discharge process due to thermal loss to the ambient and to the out flowing hot oil to the cooking unit. The temperature of oil flowing to the cooking unit increases at a decreasing rate for discharge flow rates of 2.8 g/s and 6.5 g/s. For the 2.1 g/s and 0.5 g/s mass flow rates, the temperature of the incoming oil increased and decreased abruptly before attaining a steady temperature due to the incoming hot oil and thermal absorption to the cooking unit, respectively. The temperature of oil flowing from the cooking unit to the drainage tank increases steadily for high flow rates while for low flow rates it increases at a decreasing rate to a steady value. The water temperature in the cooking pot increased from ambient to boiling point of 95.4 °C except for the 0.5 g/s mass flow rate. The temperature of water in the cooking pot increased steadily for the high discharge flow rates of 2.8 g/s and 6.5 g/s while for the 2.1 g/s mass flow rate it increased at a decreasing rate to the boiling point. Boiling could not be achieved for the 0.5 g/s discharge flow rate because more energy was lost to the ambient than conveyed to the water.

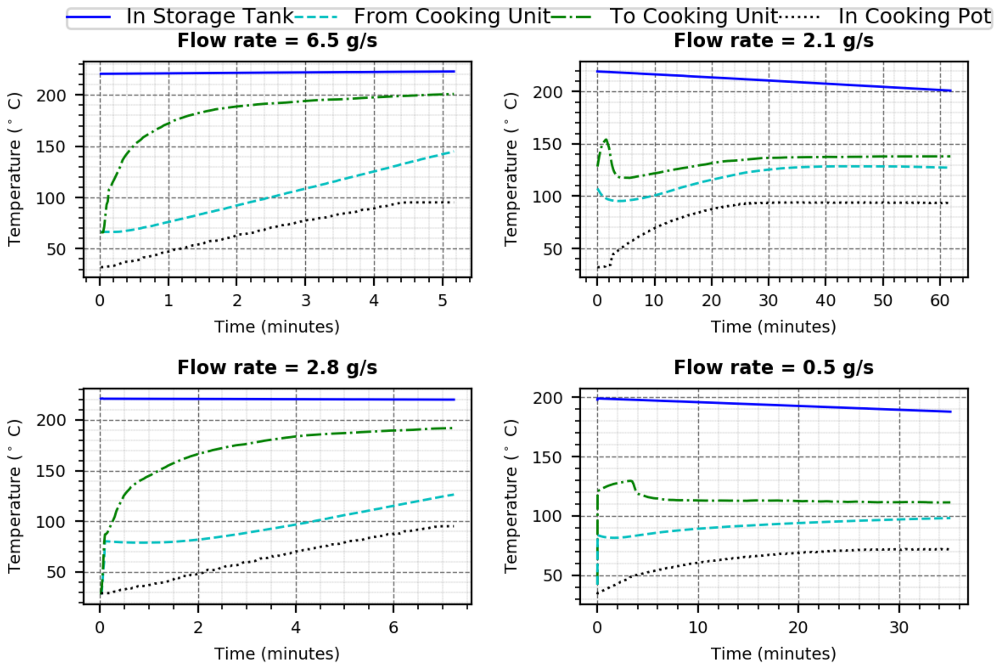

Figure 6: The temperature profiles of the oil in the storage tank, to the cooking unit, from the cooking unit and of water in the cooking pot for the discharge flow rates of 0.5 g/s, 2.1 g/s, 2.8 g/s and 6.5 g/s.

The discharge thermal power and thermal transfer efficiency

The storage tank delivered thermal energy by letting hot oil flow from it to the drainage tank through the cooking unit when valve 2 was opened. Equation (1) and equation (4) provide the values of stored thermal energy and power discharged by the storage tank respectively. The expressions for the thermal power supplied to, absorbed by and rejected by the cooking unit were obtained by modifying equation (4) as shown in Table 3. The cooking power was estimated as the ratio of the energy required to heat water from ambient ($T_a = 25\,°C$) to water temperature T_{water} to the time, *t*, taken to attain that temperature. Figure 7 shows the variation of the supplied thermal power, P_s, absorbed thermal power, P_a, rejected thermal power, P_l and the cooking power, P_c for the four mass flow rates.

Table 3: Showing how supplied, absorbed, lost and cooking thermal powers were defined

Power	Expression
Supplied thermal power at the cooking unit (W)	$P_s = c_{av}\,\rho_{av}\,v_{disc}\left(T_{in} - T_a\right)$
Absorbed thermal power by the cooking unit (W)	$P_a = c_{av}\,\rho_{av}\,v_{disc}\left(T_{in} - T_{out}\right)$
Lost thermal power by the cooking unit (W)	$P_l = c_{av}\,\rho_{av}\,v_{disc}\left(T_{out} - T_a\right)$
Cooking power at the cooking unit (W)	$P_c = \dfrac{c_{av}\,\rho_{av}\left(T_{water} - T_a\right)}{t}$

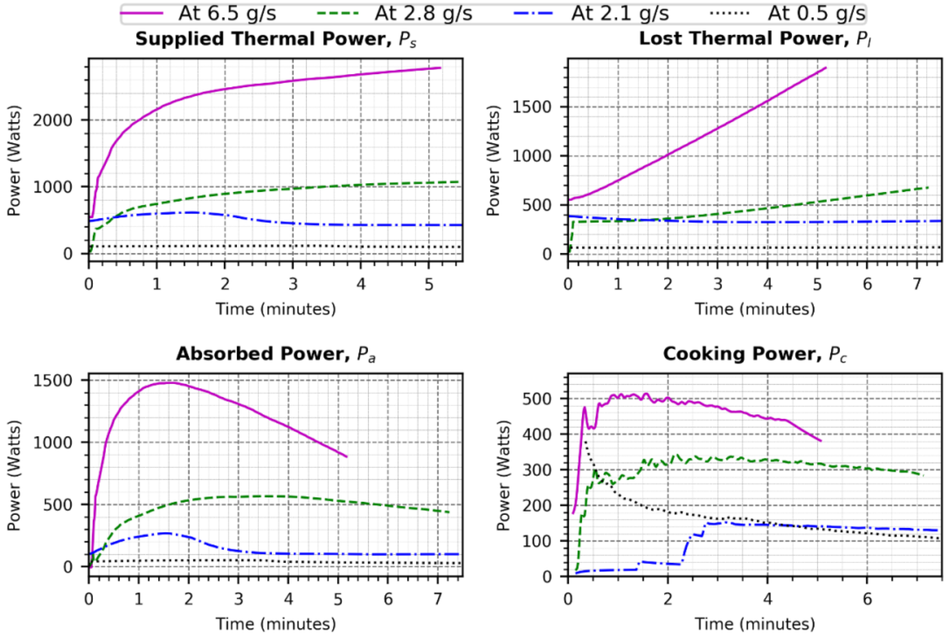

Figure 7: The variation of the thermal power supplied to, absorbed by and rejected by the cooking unit and the effective cooking power at the cooking pot for the mass flow rates of 6.5 g /s, 2.8 g /s, 2.1 g /s and 0.5 g /s.

Figure 7 shows that P_s increases at a decreasing rate which indicates that the energy source is limited. P_l, increases with the discharge flow rate. Hence P_a had peak values for each flow rate which were also reflected in the cooking power. Previous research has also reported similar maximum power point trends in systems where oil is pumped though a closed circuit (Mawire 2018). The ratio of the peak values in cooking power to the corresponding peak value in absorbed power gave the heat transfer efficiency of the cooking unit for each flow rate as shown in Table 4.

The low efficiency at the high flow rate of 6.5 g/s was due to mismatch between the rate of energy supply and absorption. For the 6.5 and 2.8 g/s, there is negligible time lag between absorbing the thermal energy and the corresponding rise in water temperature. This response time is a measure of the time it takes to transfer the heat absorbed by the cooking unit to the water in the cooking pot and needs to be small for efficient thermal transfer processes. This also explains the low heat transfer efficiency of 48.3% at the 2.1 g/s flow rate where there was a time lag of about 1.5 minutes.

Table 4: Maximum thermal absorption power points and thermal transfer efficiencies during the discharge process

Flow rate	Maximum absorbed power points	Maximum cooking power points	Thermal transfer efficiency (%)
6.5 g/s	1500 W after 1.5 min	520 W after 1.5 min	34.7%
2.8 g/s	590 W after 3.5 min	340 W after 3.5 min	57.6%
2.1 g/s	290 W after 1.5 min	140 W after 3.0 min	48.3%

Discharging efficiency

Equation (1) gives the total energy, P_w, required to raise the temperature of 0.5 litres of water from ambient temperature (25 °C) to boiling point (95.4 °C) as 40.9 Wh. This energy is delivered to the cooking pot at a given flow rate in a certain time (boiling time). Figure 5 shows that at 6.5 g/s flow rate, it takes 4.4 minutes to boil 0.5 litres of water in the cooking pot. This energy, P_w is contained in 1716 g (6.5 g/s x 4.4 x 60 s) of the incoming oil to the cooking unit. Using the equations in Table 3, the values of P_s, P_l, P_a for the incoming oil at 200 °C, lost oil at 150 °C were 203.4 Wh, 145.3 Wh and 58.1 Wh, respectively for the 6.5 g/s mass flow rate. The discharge efficiency was estimated as the ratio of P_w to P_s. Table 5 shows the results of repeating the process and the obtained discharge efficiencies for each flow rate.

Table 5 shows that the obtained discharge efficiency varied in the range 15.3– 34.7% for the mass flow rates in the range of 2.1–6.5 g/s. Discharge efficiencies can be either for the whole discharge process or for only the TES system. For the 3 tank TES system, we were interested in the efficiency of the whole discharge process and this is affected by any intermediate process or component involved. For instance, the cooking unit had a heat transfer efficiency in the range 34.7–57.6% as obtained in Table 4. Hence, the obtained low discharge efficiency can be improved by ensuring minimal heat loss occur during transfer of the hot oil to the cooking unit and using an energy efficient cooking unit (heat exchanger). The available literature considers discharge efficiency of a TES system defined as the ratio of the cumulative energy delivered by the oil leaving the TES system to the initial energy stored in the TES system (Mawire et al. 2010). Discharge efficiencies of a TES system were obtained as 39% and 48% for a system where oil is pumped through the storage tank (Mawire et al. 2010). These discharge efficiencies from literature are higher because they consider only energy supplied to the cooking unit and not to the food being cooked when compared to the 3 tank TES system.

Table 5: Summary of the discharge efficiency during the discharge process. 1 kWh = 3.6 MJ.

Flow rates (g/s)	**6.5**	**2.8**	**2.1**
Boiling time in (minutes)	4.4	6.9	29
Oil quantity needed to boil water (kg)	1.72	1.16	3.83
Temperature of the incoming oil in °C	200.0	180.0	140.0
Temperature of the outgoing oil in °C	150.0	125.0	130.0
Total thermal energy in the oil, P_s (Wh)	203.4	117.7	267.8
Average discharge efficiency	20.1%	34.7%	15.3%

Sizing an oil-based TES system

To enhance the acceptance of the TES system, its sizing for specific energy utilization, needs to be established. The minimum energy required to cook 1 kg of rice, 1 kg of raw potato and 1 kg of goat meat is 32.35 Wh, 15.59 Wh and 46.03 Wh, respectively (De et al. 2014).

For the 3-tank oil based TES system to provide a specific cooking energy, the volume of oil required, the oil temperature and efficiency of the discharge process needs to be established. The mass of oil, *m*, needed to supply the energy Q_{cook} required to cook a meal can be estimated using equation (6). Equation (6) was obtained by equating Q_{cook} to the product of the efficiency and the energy given by equation (1).

$$m = \rho V = \frac{Q_{cook}}{\eta c_{av}\left(T - T_a\right)} \qquad (6)$$

The values in Table 5 show that each mass flow rate would require a different quantity of oil for a given oil temperature. By considering 1 kg of rice to be cooked by hot oil at temperatures 150 °C or 200 °C, the estimated quantities of the required oil were given in Table 6. Table 6 shows that to cook 1 kg of rice we would need 1.14–2.66 kg of oil at 150 °C or 0.81–1.90 kg of oil at 200 °C for the oil flow rates in the range 2.1–6.5 g/s.

Table 6: Sizing an oil based TES system: Estimating the oil quantity required to cook 1 kg of rice (32.35 Wh).

Flow rates (g/s)	**6.5**	**2.8**	**2.1**
Efficiency	20.1%	34.7%	15.3%
Required oil quantity at T = 150 °C in g	1901.5	1137.7	2660.8
Required oil quantity at T = 200 °C in g	1358.2	812.7	1900.6

Solar concentrator and the mechanical thermostat

The energy source in our experiment has been electric for testing purposes though in practice a suitable renewable energy source like solar could be used. Solar energy is available intermittently with a mean solar radiation of 5.1 kWh/m^2 per day on a horizontal surface (Asere and Adeyemi 2014). This solar energy can be converted to thermal energy for cooking purposes using solar concentrators at energy efficiencies in the range 8.90–53.45% (Kaushik and Gupta 2008, Mbodji and Hajji 2016). There are different designs of solar concentrators but for heating oil in a pipe, a parabolic trough is preferred. The developed mechanical thermostat could be incorporated into a parabolic trough concentrator as shown in Figure 8.

Figure 8 shows that with the solar concentrator in the sun, the oil gets hot and flows to the heating chamber due to density difference. The oil flows along the oil flow loop continuously while in the sunshine till the desired preset oil temperature in the heating chamber is attained. At the preset oil temperature, the slider-valve opens letting hot oil flow into the storage tank as cold oil flows into the oil flow loop from the cold oil reservoir so as to maintain the oil level.

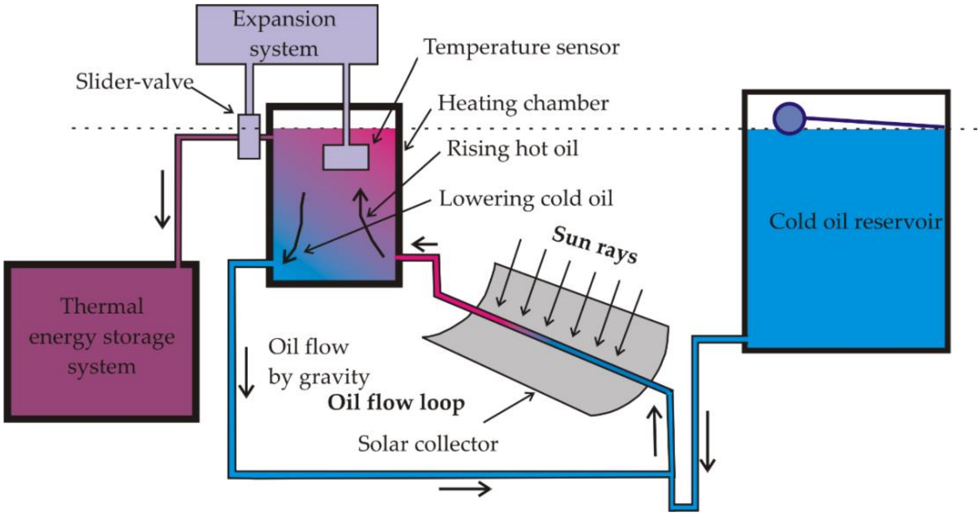

Figure 8: The schematic diagram showing how the mechanical thermostat could be connected to the cold-oil reservoir, solar concentrator and the TES system.

Conclusions

The proposed 3-tank TES system was constructed and the charging and discharging processes evaluated experimentally. The results showed that thermal charging efficiencies of 51.3% and 90% were obtained using a mechanical thermostat and an embedded heater, respectively. The adopted cooking unit exhibited a heat transfer efficiency range of 34.7–57.6%. The discharge efficiency at the flow rates of 2.1, 2.8 and 6.5 g/s varied in the range 15.3–34.7%. The proposed energy sizing approach showed that 1 kg of rice could be cooked by 1.14–2.66 kg or 0.8–1.9 kg of oil at 150 °C or 200 °C, respectively.

The charging efficiency can be improved by including the thermal energy source within or very close to the storage tank. To enhance being able to cook within 24 hours after charging the insulation of the storage tank needs to be improved: by ensuring that the insulator material is not compressed, constructing the storage tank from non-conducting materials or disengaging the storage tank from the rest of the parts when not in use. When the mechanical thermostat is not in use for some time, air gets into it making its response to temperature changes inappropriate hence air-tightness of the expansion system needs to be improved.

Acknowledgement

The authors are grateful to the Norwegian Agency for Development Cooperation (NORAD) for financially supporting this research through the Energy and Petroleum (EnPe 5) project.

References

Asere AA and Adeyemi KO 2014 A review of the energy situation in Uganda. *Int. J. Sci. Res. Pub.* 4(1).

BPS Shell 2021 Safet data sheet; Shell thermia B. http://downloads.consumables.com/doc/msds/100-0590_SDS.pdf Accessed 27/02/2021

De DK, Nathaniel M, and Olawole O 2014 Cooking with minimum energy and protection of environments and health. *IERI Procedia* 9: 148-155.

Dincer I 1999 Evaluation and selection of energy storage systems for solar thermal applications. *Int. J. Energy Res.* 23: 1017-1028.

Duffie JA and Beckman WA 2013 *Solar Engineering of Thermal Processes,* John Wiley & Sons, New York.

Fay R, Treloar G and Iyer-Raniga U 2000 Life-cycle energy analysis of buildings: a case study. *Build. Res. Inf.* 28: 31-41.

Fernandez-Seara J, Uhı FJ and Sieres J 2007 Experimental analysis of a domestic electric hot water storage tank. Part II: dynamic mode of operation. *Appl. Therm. Eng.* 27(1): 137-144.

Gadonneix P, de Castro F, de Medeiros N, Drouin R, Jain C, Kim Y, Ferioli J, Nadeau M, Sambo A, Teyssen J and Naqi A 2010 2010 survey of energy resources. *London: World Energy Council* p. 593.

Geller HS 1982 Fuel efficiency and performance of traditional and innovative cookstoves. *Proc. Indian Acad. Sci. C: Eng. Sci.* 5: 373-93.

Haller M, Cruickshank C, Streicher W, Harrison S, Andersen E and Furbo S 2009 Methods to determine stratification efficiency of thermal energy storage processes–review and theoretical comparison. *Sol. Energy* 83: 1847-1860.

Hassan RM and Hertzler G 1988 Deforestation from the overexploitation of wood resources as a cooking fuel. A dynamic approach to pricing energy resources in Sudan. *Energy Econ.* 10: 163-68.

Incropera FP, Lavine AS, Bergman TL and DeWitt DP 2007 *Fundamentals of heat and mass transfer* (Wiley), 6th ed, John Wiley & sons, New York.

Kajumba PK, Okello D, Nyeinga K and Nydal OJ 2020 Experimental investigation of a cooking unit integrated with thermal energy storage system. *J. Energy Storage* 32: 101949.

Kaushik SC and Gupta MK 2008 Energy and exergy efficiency comparison of community-size and domestic-size paraboloidal solar cooker performance. *Energy Sustain. Dev.* 12: 60-64.

Lee LY 2013 Household energy mix in Uganda. *Energy Economics* 39: 252-61.

Lugolole R, Mawire A, Lentswe KA, Okello D and Nyeinga K 2018 Thermal performance comparison of three sensible heat thermal energy storage systems during charging cycles. *Sustain. Energy Technol. Assess.* 30: 37-51.

Mawire A, McPherson M and Van den Heetkamp RRJ 2010 Discharging simulations of a thermal energy storage (TES) system for an indirect solar cooker. *Sol. Energy Mater. Sol. Cells* 94: 1100-1106.

Mawire A 2018 Experimental energy and exergy analyses of a discharging heat exchanger for a small hot-oil domestic storage tank. *Int. J. Green Energy* 15: 305-313.

Mawire A, Phori A and Taole S 2014 Performance comparison of thermal energy storage oils for solar cookers during charging. *Appl. Therm. Eng.* 73: 1323-1331.

Mbodji N and Hajji A 2016 Performance testing of a parabolic solar concentrator for solar cooking. *J. Sol. Energy Eng.* 138: 4.

Mussard M and Nydal O 2013 Charging of a heat storage coupled with a low-cost small-scale solar parabolic trough for cooking purposes. *Sol. Energy* 95: 144-154.

Nkhonjera L, Bello-Ochende T, John G and King'ondu CK 2017 A review of thermal energy storage designs, heat storage materials and cooking performance of solar cookers with heat storage. *Renew. Sustain. Energy Rev.* 75: 157-167.

Okello D, Nydal OJ, Nyeinga K and Banda EJKB 2016 Experimental investigation on heat extraction from a rock bed heat storage system for high temperature applications. *J. Energy S. Afr.* 27: 30-37.

Panwar NL, Kaushik SC and Kothari S 2012 State of the art of solar cooking: An overview. *Renew. Sustain. Energy Rev.* 16: 3776-3785.

Rehfuess E and WHO (World Health Organization) 2006 *Fuel for life: household energy and health.* WHO.

Sjogren OS and Steen AB 2018 Mechanical temperature control of oil based heat storage. Msc Dissertation, Norwegian University of Science and Technology.

Tabu B, Nyeinga K, Chaciga J and Okello D 2018 Thermal performance of selected oils in Uganda for indirect solar domestic cooking applications *Tanz. J. Sci.* 44(4): 77-90.

Villasmil W, Fischer LJ and Worlitschek J 2019 A review and evaluation of thermal insulation materials and methods for thermal energy storage systems'. *Renew. Sustain. Energy Rev.* 103: 71-84.